Available online at www.sciencedirect.com
ScienceDirect
Physica D 237 (2008) 2391–2410
PHYSICA D
www.elsevier.com/locate/physd

Quantized vortex stability and interaction in the nonlinear wave equation

Weizhu Bao[a,b,*], Rong Zeng[c], Yanzhi Zhang[a,1]

[a] Department of Mathematics, National University of Singapore, Singapore 117543, Singapore
[b] Center for Computational Science and Engineering, National University of Singapore, Singapore 117543, Singapore
[c] Department of Electrical Engineering, Tsinghua University, Beijing, 100084, China

Received 28 May 2007; received in revised form 11 March 2008; accepted 19 March 2008
Available online 25 March 2008

Communicated by B. Sandstede

Abstract

The stability and interaction of quantized vortices in the nonlinear wave equation (NLWE) are investigated both numerically and analytically. A review of the reduced dynamic law governing the motion of vortex centers in the NLWE is provided. The second order nonlinear ordinary differential equations for the reduced dynamic law are solved analytically for some special initial data. Using 2D polar coordinates, the transversely highly oscillating far field conditions can be efficiently resolved in the phase space, thus giving rise to an efficient and accurate numerical method for the NLWE with non-zero far field conditions. By applying this numerical method to the NLWE, we study the stability of quantized vortices and find numerically that the quantized vortices with winding number $m = \pm 1$ are dynamically stable, and resp. $|m| > 1$ are dynamically unstable, in the dynamics of NLWE. We then compare numerically quantized vortex interaction patterns of the NLWE with those from the reduced dynamic law qualitatively and quantitatively. Some conclusive findings are obtained, and discussions on numerical and theoretical results are made to provide further understanding of vortex stability and interactions in the NLWE. Finally, the vortex motion under an inhomogeneous potential in the NLWE is also studied.

Keywords: Nonlinear wave equation; Quantized vortex; Reduced dynamic law; Stability; Vortex interaction

1. Introduction

In this paper we study quantized vortex stability and interaction in the nonlinear wave equation (NLWE) [26,22]:

$$\partial_{tt}\psi(\mathbf{x},t) = \nabla^2\psi + \frac{1}{\varepsilon^2}\left(V(\mathbf{x}) - |\psi|^2\right)\psi, \quad \mathbf{x}\in\mathbb{R}^2, \quad t>0, \tag{1.1}$$

with initial conditions

$$\psi(\mathbf{x},0) = \psi_0(\mathbf{x}), \qquad \partial_t\psi(\mathbf{x},0) = \psi_1(\mathbf{x}), \quad \mathbf{x}\in\mathbb{R}^2 \tag{1.2}$$

and nonzero far field conditions

$$|\psi(\mathbf{x},t)| \to 1, \ (\text{e.g.}\psi \to \mathrm{e}^{\mathrm{i}m\theta}), \quad t\geq 0, \quad \text{when } r = |\mathbf{x}| = \sqrt{x^2+y^2} \to \infty. \tag{1.3}$$

Here t is time, $\mathbf{x} = (x, y)^{\mathrm{T}} \in \mathbb{R}^2$ is the Cartesian coordinate vector, (r, θ) is the polar coordinate system, $\psi = \psi(\mathbf{x}, t)$ is a complex-valued order parameter (or wave function), $V(\mathbf{x})$ is a real-valued external potential satisfying $\lim_{|\mathbf{x}|\to\infty} V(\mathbf{x}) = 1$, $m \in \mathbb{Z}$ is a given integer and $\varepsilon > 0$ is a constant.

It is well known that there exist stationary *vortex solutions* with the single winding number (or index) $m \in \mathbb{Z}$ of the NLWE (1.1) with $\varepsilon = 1$ and $V(\mathbf{x}) \equiv 1$ [25,22,14], which take the form

$$\phi_m(\mathbf{x}) = f_m(r)\,\mathrm{e}^{\mathrm{i}m\theta}, \quad \mathbf{x} = (r\cos\theta, r\sin\theta)^{\mathrm{T}} \in \mathbb{R}^2, \tag{1.4}$$

where the modulus $f_m(r)$ is a real-valued function satisfying

$$\frac{1}{r}\frac{\mathrm{d}}{\mathrm{d}r}\left(r\frac{\mathrm{d}f_m(r)}{\mathrm{d}r}\right) - \frac{m^2}{r^2}f_m(r) + \left(1 - f_m^2(r)\right)f_m(r) = 0,$$

* Corresponding author at: Department of Mathematics, National University of Singapore, Singapore 117543, Singapore. Tel.: +65 6516 2765; fax: +65 6774 6756.
E-mail addresses: bao@math.nus.edu.sg (W. Bao), zengrong@tsinghua.edu.cn (R. Zeng), yzhang@scs.fsu.edu (Y. Zhang).
URL: http://www.math.nus.edu.sg/~bao/ (W. Bao).
[1] Current address: School of Computational Science, Florida State University, Tallahassee, FL 32306-4120, USA.

0167-2789/$ - see front matter © 2008 Elsevier B.V. All rights reserved.
doi:10.1016/j.physd.2008.03.026

$$0 < r < \infty, \tag{1.5}$$

$$f_m(0) = 0, \qquad f_m(r) = 1, \quad \text{when } r \to \infty. \tag{1.6}$$

Numerical solutions of the modulus for different winding numbers m were reported in the literature [25,34,35] by solving the boundary value problem (1.5)–(1.6) numerically. In addition, the core size r_m^0 of a vortex state with winding number m is defined by the condition $f_m(r_m^0) = 0.755$, and then when $m = \pm 1$, the core size $r_1^0 \approx 1.75$ [34,35]. In fact, the quantized vortex state (1.4) satisfying the nonzero far field condition (1.3) is usually called as "bright-tail" vortex which was also widely studied in superfluid Helium [25,12,22,23,5,34,35], superconductors [25,22,15,34,35], etc. On the other hand, the quantized vortex state (1.4) decaying to zero at far field, i.e.

$$|\psi(\mathbf{x}, t)| \to 0, \quad t \geq 0, \text{ when } r \to \infty, \tag{1.7}$$

is usually called the "dark-tail" vortex, and has been widely studied in Bose–Einstein condensation in trapped atomic gases at ultra-low temperatures [3,24,21,1,10,9,8,17,18,36], nonlinear optics [31,32], etc.

Quantized vortices have a long history that begins with the study of liquid Helium and superconductors. Their appearance is viewed as a typical signature of superfluidity which describe a phase of matter characterized by the complete absence of viscosity. The examples of superfluidity can be found in liquid Helium, Bose–Einstein condensation, superconductivity and nonlinear optics, etc. In 1955, Feynman [13] made the prediction that a superfluid rotation may be subject to an array of quantized singularities, namely, the quantized vortices. The seminal work of Abrikosov [2] in 1957 already made predictions of the vortex lattice in superconductors a decade before the experimental confirmation. Research on the quantized vortex phenomena has since flourished and it was recently highlighted by the Nobel Prizes in Physics awarded to Cornell, Weimann and Ketterle in 2001 and to Ginzburg, Abrikosov and Leggett in 2003, who have made decisive contributions to Bose–Einstein condensation, superfluidity and superconductivity and to the understanding of the quantized vortex states. In recent years, there have been many works on the numerical simulations and mathematical analysis for quantized vortex states in superfluidity and superconductivity. It is truly remarkable that many of the phenomenological properties of quantized vortices have been well captured by relatively simple mathematical models, for example, the Gross–Pitaesvkii equations [29,7] and the Ginzburg–Landau equations [11,4]. The structures of quantized vortex states have been studied through various approaches ranging from asymptotic analysis, numerical simulations and rigorous mathematical analysis. Despite the great progress made in the last decade on quantized vortex states in superfluidity and superconductivity, it should be pointed out that the efficient computation and rigorous mathematical study of a large part of the subject on vortex dynamics and interaction remains nearly non-existent. Indeed, what has become available in the literature are primarily studies of the various dynamical laws of well separated vortices deduced from the Ginzburg–Landau–Schrodinger equations [25,12,23,34,35,16,27,28,20,33] or the Gross–Pitaevskii equation with weak interaction [19,30]. On the other hand, numerical simulations have become useful tools that could help in providing a more clear picture on the exotic vortex dynamics and interaction driven by various forces, even though there are also challenging computational issues to be tackled. Thus understanding numerically and mathematically the dynamics and interaction of quantized vortices in superfluidity and superconductivity bears tremendous importance both scientifically and technologically.

The aim of this paper is first to study numerically the stability of quantized vortex solutions (1.4) of NLWE and then to investigate analytically and numerically the interaction patterns of several quantized vortices with winding number $m = \pm 1$ in NLWE, i.e., we study (1.1) with initial conditions in (1.2) containing several vortices, which take the form

$$\psi_0(\mathbf{x}) = \prod_{j=1}^{N} \phi_{m_j}\left(\mathbf{x} - \mathbf{x}_j^0\right) = \prod_{j=1}^{N} \phi_{m_j}\left(x - x_j^0, y - y_j^0\right), \quad \mathbf{x} \in \mathbb{R}^2. \tag{1.8}$$

Here N is the total number of vortices, ϕ_{m_j} is the vortex state in (1.4) with winding number $m_j = \pm 1$ (see [25,34] for their numerical solutions), and $\mathbf{x}_j^0 = (x_j^0, y_j^0)^{\mathrm{T}}$ is the initial location of the j-th $(1 \leq j \leq N)$ vortex center. That is, we consider the interaction of N vortices by shifting their initial centers from the origin $(0, 0)^{\mathrm{T}}$ to $\mathbf{x}_j^0$ $(1 \leq j \leq N)$. Taking $m = \sum_{j=1}^{N} m_j$ in (1.3), we refer to vortices with the same winding numbers as *like vortices* while those with different winding numbers as *opposite vortices*.

In fact, vortex dynamics for NLWE is a typical model of the "particle and field" theories of classical physics. The formal derivation of the reduced dynamic law was done by Neu [26] for NLWE (1.1) with $\varepsilon = 1$ and $V(\mathbf{x}) \equiv 1$. In this case, for N well-separated vortices of winding numbers $m_j = \pm 1$ $(1 \leq j \leq N)$, he obtained asymptotically the following second order nonlinear ordinary differential equations (ODEs) for the reduced dynamic law governing the induced motion of the N vortex centers $\mathbf{x}_j(t)$ $(1 \leq j \leq N)$ in the leading order, i.e. the adiabatic approximation [26], as

$$\kappa\, \mathbf{x}_j''(t) = 2m_j \sum_{l=1, l\neq j}^{N} m_l \frac{\mathbf{x}_j(t) - \mathbf{x}_l(t)}{|\mathbf{x}_j(t) - \mathbf{x}_l(t)|^2}, \quad t \geq 0, \tag{1.9}$$

$$\mathbf{x}_j(0) = \mathbf{x}_j^0, \qquad \mathbf{x}_j'(0) = \mathbf{x}_j^1, \quad 1 \leq j \leq N, \tag{1.10}$$

where κ is a constant determined from the initial setup (1.8). He also made an interesting connection between vortex dynamics and the Dirac theory of electrons [26]. Later, Lin [22] gave a rigorous mathematical proof of the reduced dynamic law with a correction term denoting the residuals of a holomorphic function defined away from the vortices. Here we will solve the second order nonlinear ODEs (1.9) for some special initial data in (1.10). These solutions will provide qualitatively the interaction patterns of quantized vortices in NLWE. By proposing an efficient and accurate numerical method for

NLWE, we can also study numerically vortex interaction patterns by directly simulating NLWE and compare them with those from the reduced dynamic law qualitatively and quantitatively.

The paper is organized as follows. In Section 2, based on the second order nonlinear ODEs of the reduced dynamic law, we prove the conservation of the mass center and mean velocity of the N vortex centers under certain conditions, and solve analytically the reduced dynamic law with a few types of initial data. In Section 3, an efficient and accurate numerical method is proposed for simulating NLWE and the stability of quantized vortices is reported. In Section 4, the interactions of quantized vortices in NLWE with zero initial velocity are obtained by directly simulating (1.1) and compared with those from the reduced dynamic law. In Section 5, the interactions of quantized vortices with nonzero initial velocity and the dynamics of vortex state under an inhomogeneous external potential are reported. Finally, some conclusions are drawn in Section 6.

2. The reduced dynamic law and its solutions

In this section, we first prove the conservation of the mass center and mean velocity of the N vortex centers in the reduced dynamic law (1.9) under certain conditions. These conservation properties can be used to solve the dynamic law in special cases and to compare with the direct numerical simulation of NLWE. We then solve the second order nonlinear ODEs (1.9)–(1.10) analytically for several types of initial data, and such analytical solutions can again be compared with the numerical solutions of NLWE.

2.1. Conservation laws

Define respectively the mass center $\overline{\mathbf{x}}(t)$ and the mean velocity $\overline{\mathbf{v}}(t)$ of the N vortex centers as

$$\overline{\mathbf{x}}(t) := \frac{1}{N}\sum_{j=1}^{N}\mathbf{x}_j(t), \quad \text{and}$$
$$\overline{\mathbf{v}}(t) := \overline{\mathbf{x}}'(t) = \frac{1}{N}\sum_{j=1}^{N}\mathbf{x}_j'(t). \tag{2.1}$$

Then we have

Lemma 2.1. *The mean velocity of the N vortex centers in the reduced dynamic law (1.9) for NLWE is conserved, i.e.*

$$\overline{\mathbf{v}}(t) := \frac{1}{N}\sum_{j=1}^{N}\mathbf{x}_j'(t) \equiv \overline{\mathbf{v}}(0) := \frac{1}{N}\sum_{j=1}^{N}\mathbf{x}_j'(0) = \frac{1}{N}\sum_{j=1}^{N}\mathbf{x}_j^1, \quad t \geq 0. \tag{2.2}$$

In addition, the dynamics of the mass center of the N vortices in the reduced dynamic law (1.9) for NLWE satisfies

$$\overline{\mathbf{x}}(t) := \frac{1}{N}\sum_{j=1}^{N}\mathbf{x}_j(t) = \overline{\mathbf{x}}(0) + t\,\overline{\mathbf{v}}(0) = \frac{1}{N}\sum_{j=1}^{N}\mathbf{x}_j^0 + t\left(\frac{1}{N}\sum_{j=1}^{N}\mathbf{x}_j^1\right), \quad t \geq 0, \tag{2.3}$$

which immediately implies that the mass center is conserved if $\overline{\mathbf{v}}(0) = 0$, and respectively, it moves to infinity starting from the initial mass center $\overline{\mathbf{x}}(0)$ along the direction of the initial mean velocity $\overline{\mathbf{v}}(0)$ if $\overline{\mathbf{v}}(0) \neq 0$.

Proof. Summing (1.9) for $1 \leq j \leq N$ and noticing (2.1), we get for $t \geq 0$,

$$\begin{aligned}\overline{\mathbf{v}}'(t) &= \overline{\mathbf{x}}''(t) = \frac{1}{N}\sum_{j=1}^{N}\mathbf{x}_j''(t)\\ &= \frac{1}{N}\sum_{j=1}^{N}\frac{2m_j}{\kappa}\sum_{l=1,l\neq j}^{N} m_l\frac{\mathbf{x}_j(t)-\mathbf{x}_l(t)}{|\mathbf{x}_j(t)-\mathbf{x}_l(t)|^2}\\ &= \frac{2}{\kappa N}\sum_{j=1}^{N-1}\sum_{j<l\leq N} m_j m_l\\ &\quad\times\left[\frac{\mathbf{x}_j(t)-\mathbf{x}_l(t)}{|\mathbf{x}_j(t)-\mathbf{x}_l(t)|^2}+\frac{\mathbf{x}_l(t)-\mathbf{x}_j(t)}{|\mathbf{x}_l(t)-\mathbf{x}_j(t)|^2}\right]\\ &= 0, \quad t \geq 0.\end{aligned} \tag{2.4}$$

Thus the conservation of the mean velocity in (2.2) is a combination of the above and (1.10). Plugging (2.2) into (2.1), we obtain

$$\overline{\mathbf{x}}'(t) = \overline{\mathbf{v}}(t) \equiv \overline{\mathbf{v}}(0), \quad t \geq 0. \tag{2.5}$$

Integrating the above and noticing (1.10), we get (2.3) immediately. □

2.2. Analytical solutions of the reduced dynamic law

Noticing (2.2) and (2.3), we can solve the second order nonlinear ODEs (1.9) analytically for some special initial data in (1.10). Without loss of generality, in these cases, we assume that the initial mass center is at the origin, i.e. $\overline{\mathbf{x}}(0) = (0,0)^{\mathrm{T}}$, and denote θ_0 as a given constant and $m_0 = +1$ or -1.

Lemma 2.2. *If the initial data in (1.10) satisfies for $1 \leq j \leq N$*

$$\mathbf{x}_j^0 = a\left(\cos\left(\frac{2j\pi}{N}+\theta_0\right), \sin\left(\frac{2j\pi}{N}+\theta_0\right)\right)^{\mathrm{T}}, \quad \mathbf{x}_j^1 = (0,0)^{\mathrm{T}}, \quad m_j = m_0, \tag{2.6}$$

*i.e. the N ($N \geq 2$) like vortices are uniformly located on a circle and there is no initial velocity (denoted as **Pattern I**), then the solutions of (1.9)–(1.10) can be given, for $1 \leq j \leq N$ with $N \geq 2$, by*

$$\begin{aligned}\mathbf{x}_j(t) &= c_N(t)\left(\cos\left(\frac{2j\pi}{N}+\theta_0\right), \sin\left(\frac{2j\pi}{N}+\theta_0\right)\right)^{\mathrm{T}}\\ &= \frac{c_N(t)}{a}\mathbf{x}_j^0, \quad t \geq 0,\end{aligned} \tag{2.7}$$

where $c_N(t)$ satisfies the following second order ODE

$$c_N''(t)c_N(t) = \frac{N-1}{\kappa}, \quad t \geq 0, \quad c_N(0) = a, \quad c_N'(0) = 0; \tag{2.8}$$

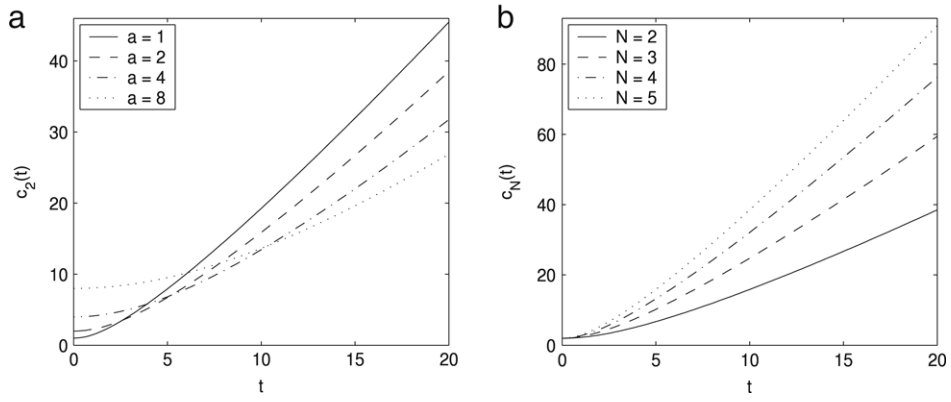

Fig. 1. Numerical solutions of the ODE (2.8) with $\kappa = 1$ for: (a) different a with $N = 2$, and (b) different N with $a = 2$.

or the following first order ODE

$$c_N'(t) = \sqrt{2(N-1)/\kappa}\sqrt{\ln[c_N(t)/a]}, \quad t \geq 0, \qquad c_N(0) = a. \tag{2.9}$$

Proof. For simplicity, we first consider the case of $N = 2$. By conservation of the mass center, we have

$$\mathbf{x}_1(t) = -\mathbf{x}_2(t), \quad t \geq 0. \tag{2.10}$$

Plugging (2.10) into (1.9) with $N = 2$, we get for $1 \leq j \leq 2$

$$\kappa \mathbf{x}_j''(t) = \frac{\mathbf{x}_j(t)}{|\mathbf{x}_j(t)|^2}, \quad t \geq 0, \text{ with } \mathbf{x}_j(0) = \mathbf{x}_j^0, \qquad \mathbf{x}_j'(0) = \mathbf{x}_j^1 = (0,0)^{\mathrm{T}}. \tag{2.11}$$

Based on the structure of the ODEs (2.11), we take the ansatz for the solution as

$$\mathbf{x}_j(t) = \frac{c_2(t)}{a}\mathbf{x}_j^0, \quad t \geq 0, 1 \leq j \leq 2, \tag{2.12}$$

where $c_2(t)$ is a function of time t satisfying $c_2(0) = a$ and $c_2'(0) = 0$. Substituting (2.12) into (2.11) and applying the dot-product at both sides by $\mathbf{x}_j^0$, noticing (2.6) with $N = 2$, we get (2.8) for $N = 2$ immediately. For the cases of $N > 2$, we can generalize the solution (2.12) as

$$\mathbf{x}_j(t) = \frac{c_N(t)}{a}\mathbf{x}_j^0, \quad t \geq 0, 1 \leq j \leq N, \tag{2.13}$$

where $c_N(t)$ is a function of time t satisfying $c_N(0) = a$ and $c_N'(0) = 0$. Substituting (2.13) into (1.9) and applying dot-product at both sides by $\mathbf{x}_j^0$, noticing (2.6), we get

$$\begin{aligned} c_N''(t) &= \frac{2}{\kappa c_N(t)} \sum_{l=1, l\neq j}^{N} m_j m_l \frac{(\mathbf{x}_j^0 - \mathbf{x}_l^0)\cdot \mathbf{x}_j^0}{|\mathbf{x}_j^0 - \mathbf{x}_l^0|^2} \\ &= \frac{2}{\kappa c_N(t)} \sum_{l=1, l\neq j}^{N} \frac{a^2 - \mathbf{x}_l^0 \cdot \mathbf{x}_j^0}{2a^2 - 2\mathbf{x}_l^0 \cdot \mathbf{x}_j^0} \\ &= \frac{N-1}{\kappa c_N(t)}, \quad t \geq 0. \end{aligned} \tag{2.14}$$

Thus, the solution (2.7) is a combination of (2.13), (2.14) and (2.6). □

Fig. 1 shows numerical results of the second order ODE (2.8) with $\kappa = 1$ for different N and a by using the standard second order finite difference discretization for (2.8). From the results in Lemma 2.2 and Fig. 1, we can see that, when the N vortices are uniformly located on a circle with zero velocity initially, by the reduced dynamic law, each vortex moves outside along the line passing through its initial location and the origin, and these N vortices are located on a circle at any time t with its radius increasing with time as $c_N(t)$ in (2.8). In addition, from our numerical results, for any $\delta > 0$, we observe that (cf. Fig. 1)

$$C_1 \frac{N-1}{a^2\kappa} t^{1-\delta} \leq c_N(t) \leq C_2 \frac{N-1}{a^2\kappa} t^{1+\delta}, \quad t \gg 1,$$

where C_1 and C_2 are two generic positive constants independent of N and a.

Lemma 2.3. *If the initial data in (1.10) satisfies*

$$\mathbf{x}_N^0 = (0,0)^{\mathrm{T}}, \qquad \mathbf{x}_N^1 = (0,0)^{\mathrm{T}}, \qquad m_N = m_0, \tag{2.15}$$

and for $1 \leq j \leq N-1$,

$$\mathbf{x}_j^0 = a\left(\cos\left(\frac{2j\pi}{N-1} + \theta_0\right), \sin\left(\frac{2j\pi}{N-1} + \theta_0\right)\right)^{\mathrm{T}}, \qquad \mathbf{x}_j^1 = (0,0)^{\mathrm{T}}, \qquad m_j = m_0, \tag{2.16}$$

*i.e. the N ($N \geq 3$) like vortices are uniformly located on a circle and its center and there is no initial velocity (denoted as **Pattern II**), then the solutions of (1.9) and (1.10) are:*

$$\mathbf{x}_N(t) \equiv (0,0)^{\mathrm{T}}, \quad t \geq 0, \tag{2.17}$$

and for $1 \leq j \leq N-1$ *with* $N \geq 3$,

$$\begin{aligned} \mathbf{x}_j(t) &= d_N(t)\left(\cos\left(\frac{2j\pi}{N-1} + \theta_0\right), \sin\left(\frac{2j\pi}{N-1} + \theta_0\right)\right)^{\mathrm{T}} \\ &= \frac{d_N(t)}{a}\mathbf{x}_j^0, \quad t \geq 0, \end{aligned} \tag{2.18}$$

where $d_N(t)$ satisfies the following second order ODE

$$d_N''(t) d_N(t) = \frac{N}{\kappa}, \quad t \geq 0, \quad d_N(0) = a, \quad d_N'(0) = 0; \tag{2.19}$$

or the following first order ODE

$$d_N'(t) = \sqrt{2N/\kappa}\sqrt{\ln[d_N(t)/a]}, \quad t \geq 0, \quad d_N(0) = a. \tag{2.20}$$

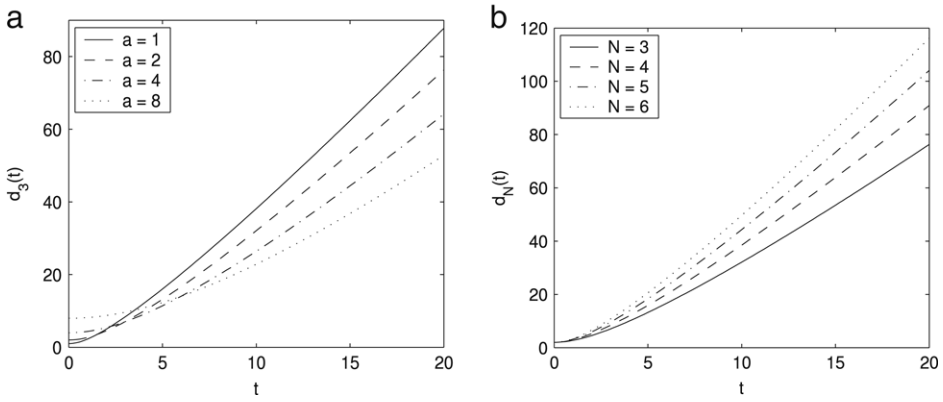

Fig. 2. Numerical solutions of the ODE (2.19) with $\kappa = 1$ for: (a) different a with $N = 3$, and (b) different N with $a = 2$.

Proof. Due to symmetry of the ODEs (1.9), the initial data (2.15)–(2.16), and the conservation of mass center (2.3) and mean velocity (2.2), we can get the solution (2.17) immediately. Similar as in the proof of Lemma 2.2, we assume

$$\mathbf{x}_j(t) = \frac{d_N(t)}{a}\mathbf{x}_j^0, \quad t \geq 0, 1 \leq j \leq N-1, \tag{2.21}$$

where $d_N(t)$ is a function of time t satisfying $d_N(0) = a$ and $d_N'(0) = 0$. Substituting (2.21) into (1.9) and applying dot-product at both sides by $\mathbf{x}_j^0$, noticing (2.16), we get

$$\begin{aligned} d_N''(t) &= \frac{2}{\kappa d_N(t)}\left[m_j m_N \frac{(\mathbf{x}_j^0 - \mathbf{x}_N^0)\cdot \mathbf{x}_j^0}{|\mathbf{x}_j^0 - \mathbf{x}_N^0|^2} + \sum_{l=1, l\neq j}^{N-1} m_j m_l \frac{(\mathbf{x}_j^0 - \mathbf{x}_l^0)\cdot \mathbf{x}_j^0}{|\mathbf{x}_j^0 - \mathbf{x}_l^0|^2}\right] \\ &= \frac{2}{\kappa d_N(t)}\left[m_0^2 + \sum_{l=1, l\neq j}^{N-1} \frac{a^2 - \mathbf{x}_l^0\cdot \mathbf{x}_j^0}{2a^2 - 2\mathbf{x}_l^0\cdot \mathbf{x}_j^0}\right] \\ &= \frac{2}{\kappa d_N(t)}\left[1 + \frac{N-2}{2}\right] \\ &= \frac{N}{\kappa d_N(t)}, \quad t \geq 0. \end{aligned} \tag{2.22}$$

Thus, the solution (2.18) is a combination of (2.21), (2.22) and (2.16). □

Fig. 2 shows numerical results of the second order ODE (2.19) with $\kappa = 1$ for different N and a. From the results in Lemma 2.3 and Fig. 2, we can see that, for the dynamics of (1.9)–(1.10) in Pattern II, by the reduced dynamic law, the vortex initially at the center of the circle does not move for any time $t \geq 0$, each of the other $N-1$ vortices moves outside along the line passing through its initial location and the origin, and these $N-1$ vortices are located on a circle at any time t with its radius increasing with time as $d_N(t)$ in (2.19). Again, from our numerical results, for any $\delta > 0$, we observe that (cf. Fig. 2)

$$C_1 \frac{N}{a^2\kappa} t^{1-\delta} \leq d_N(t) \leq C_2 \frac{N}{a^2\kappa} t^{1+\delta}, \quad t \gg 1.$$

Lemma 2.4. *If the initial data in (1.10) satisfies the same as (2.15) and (2.16) except $m_N = -m_0$ for the center vortex, i.e. the N ($N \geq 3$) opposite vortices are uniformly located on a circle and its center and there is no initial velocity (denoted as **Pattern III**), then the solutions of (1.9)–(1.10) are:*

$$\mathbf{x}_N(t) \equiv (0,0)^{\mathrm{T}}, \quad t \geq 0, \tag{2.23}$$

and for $1 \leq j \leq N-1$ with $N \geq 3$,

$$\begin{aligned} \mathbf{x}_j(t) &= g_N(t)\left(\cos\left(\frac{2j\pi}{N-1} + \theta_0\right), \sin\left(\frac{2j\pi}{N-1} + \theta_0\right)\right)^{\mathrm{T}} \\ &= \frac{g_N(t)}{a}\mathbf{x}_j^0, \quad t \geq 0, \end{aligned} \tag{2.24}$$

where $g_N(t)$ satisfies the following second order ODE

$$\begin{aligned} g_N''(t)g_N(t) &= \frac{N-4}{\kappa}, \quad t \geq 0, \quad g_N(0) = a, \\ g_N'(0) &= 0; \end{aligned} \tag{2.25}$$

or the following first order ODE

$$g_N'(t) = \alpha_N\sqrt{\ln[d_N(t)/a]}, \quad t \geq 0, \quad c_N(0) = a, \tag{2.26}$$

with

$$\alpha_N = \begin{cases} -\sqrt{2/\kappa}, & N = 3, \\ 0, & N = 4, \\ \sqrt{2(N-4)/\kappa}, & N \geq 5. \end{cases}$$

The proof follows the analogous results in Lemma 2.3. Fig. 3 shows numerical results of the second order ODE (2.25) with $\kappa = 1$ for different N and a. From the results in Lemma 2.4 and Fig. 3, we can see that, for the dynamics of (1.9) and (1.10) in Pattern III, by the reduced dynamic law: (i) the vortex initially at the origin does not move during the interaction, each of the other $N-1$ vortices moves along the line passing through its initial location and the origin, and these $N-1$ vortices are located on a circle at any time t; (ii) when $N = 3$, the two vortices with the same index move towards each other and collide with the vortex having opposite index at the origin at finite time $t = t_c$; (iii) when $N = 4$, all the four vortices do not move and stay at their initial locations for any $t \geq 0$, and (iv) when $N \geq 5$, the $N-1$ vortices with the same index move outside and they never collide with the vortex with the opposite

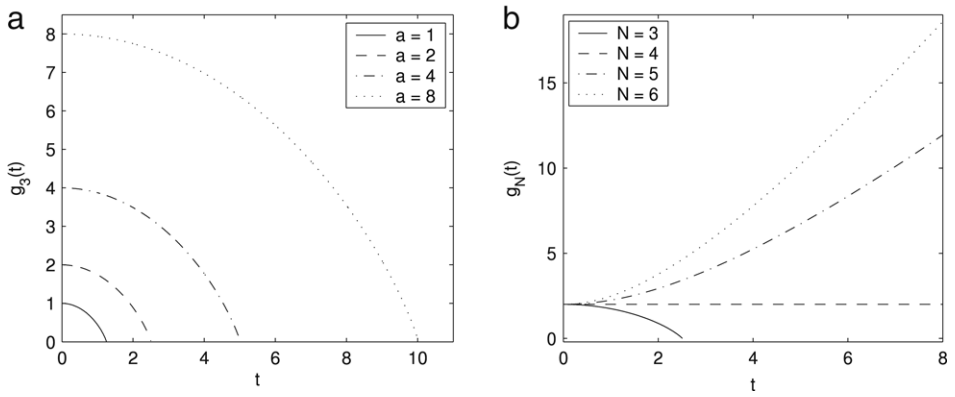

Fig. 3. Numerical solutions of the ODE (2.25) with $\kappa = 1$ for: (a) different a with $N = 3$, and (b) different N with $a = 2$.

index no matter how small the initial radius of the circle is. Again, from our numerical results, we observe that, for $N = 3$, the collision time satisfies (cf. Fig. 3(a))

$$t_c = O(a), \quad a \gg 1,$$

and for $N \geq 5$, for any $\delta > 0$, we have (cf. Fig. 3(b))

$$C_1 \frac{N-4}{a^2\kappa} t^{1-\delta} \leq g_N(t) \leq C_2 \frac{N-4}{a^2\kappa} t^{1+\delta}, \quad t \gg 1.$$

Lemma 2.5. *If the initial data in (1.10) satisfies for $j = 1, 2$*

$$\mathbf{x}_j^0 = a\,(\cos(j\pi + \theta_0), \sin(j\pi + \theta_0))^{\mathrm{T}}, \quad \mathbf{x}_j^1 = (0,0)^{\mathrm{T}}, \quad m_1 = -m_2 = m_0, \tag{2.27}$$

*i.e. two opposite vortices (denoted as **Pattern IV**), then the solutions of (1.9)–(1.10) can be given, for $j = 1, 2$, by*

$$\mathbf{x}_j(t) = h_N(t)\,(\cos(j\pi + \theta_0), \sin(j\pi + \theta_0))^{\mathrm{T}} = \frac{h_N(t)}{a}\mathbf{x}_j^0, \quad 0 \leq t \leq t_c, \tag{2.28}$$

where $h_N(t)$ satisfies the following second order ODE

$$h_N''(t) h_N(t) = -\frac{1}{\kappa}, \quad t \geq 0, \quad h_N(0) = a, \quad h_N'(0) = 0; \tag{2.29}$$

or the following first order ODE

$$h_N'(t) = -\sqrt{2/\kappa}\sqrt{\ln[h_N(t)/a]}, \quad t \geq 0, \quad h_N(0) = a. \tag{2.30}$$

The proof is similar to that of Lemma 2.2 with $N = 2$. Fig. 4 shows numerical results of the second order ODE (2.29) with $\kappa = 1$ for different a. From the results in Lemma 2.5 and Fig. 4, we can see that, for the dynamics of (1.9)–(1.10) in Pattern IV, when $0 \leq t < t_c$, the two vortices move towards each other along a line passing through their initial locations and collide at the origin at time $t = t_c$ according to the reduced dynamic law. Again, from our numerical results, we observe that the collision time satisfies (cf. Fig. 4)

$$t_c = O(a), \quad a \gg 1. \tag{2.31}$$

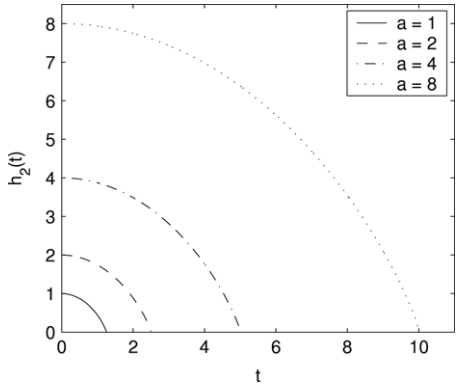

Fig. 4. Numerical solutions of the ODE (2.29) with $\kappa = 1$ for different a.

3. Numerical method and stability of vortex solutions

In this section, we first propose an efficient and accurate numerical method to discretize NLWE (1.1) with (1.2)–(1.3) and then apply it to study numerically the stability of the quantized vortex state solution (1.4) of NLWE (1.1).

3.1. An efficient and accurate numerical method

In the practical implementation, we truncate the problem (1.1)–(1.3) to one defined in a bounded computational domain with an inhomogeneous Dirichlet boundary condition:

$$\partial_{tt}\psi(\mathbf{x}, t) = \nabla^2\psi + \frac{1}{\varepsilon^2}\left(V(\mathbf{x}) - |\psi|^2\right)\psi, \quad \mathbf{x} \in \Omega_R, \quad t > 0, \tag{3.1}$$

$$\psi(\mathbf{x}, t) = \mathrm{e}^{\mathrm{i}m\theta}, \quad \mathbf{x} \in \Gamma = \partial\Omega_R, t \geq 0, \tag{3.2}$$

$$\psi(\mathbf{x}, 0) = \psi_0(\mathbf{x}), \qquad \partial_t\psi(\mathbf{x}, 0) = \psi_1(\mathbf{x}), \quad \mathbf{x} = \overline{\Omega}_R, \tag{3.3}$$

where we choose $\Omega_R = \{(x, y), r = \sqrt{x^2 + y^2} < R\}$ with R sufficiently large. In our simulations, a sufficiently large R is chosen to assure that the effect of domain truncation remains insignificant. The use of more sophisticated radiation boundary conditions is an interesting topic that remains to be examined in the future.

To match the highly oscillatory boundary condition (3.2) in the transverse direction when m is large, we use the polar coordinate (r, θ), and discretize (3.1)–(3.3) in θ-direction by

the Fourier pseudospectral method, in r-direction by finite difference or finite element method and in time by the second order central finite difference method. Choose a time step $\Delta t > 0$ and a mesh size in θ-direction $\Delta\theta = 2\pi/K > 0$ with K an even positive integer. Denote the grid points as $\theta_k = k\Delta\theta$ for $0 \le k \le K$, and time sequence as $t_n = n\Delta t$ for $n = 0, 1, \ldots$; let $0 < r_1 < r_2 < \cdots < r_J = R$ be a partition of $[r_1, R]$ and denote $r_0 = -r_1$. Let $\psi^n_{j,k}$ be the approximation of $\psi(r_j, \theta_k, t_n)$ and ψ^n be the solution vector at time $t = t_n$ with component $\psi^n_{j,k}$. Then the NLWE (3.1) can be discretized, for $1 \le j < J$, $0 \le k \le K$ and $n = 0, 1, \ldots,$ as

$$\frac{\psi^{n+1}_{j,k} - 2\psi^n_{j,k} + \psi^{n-1}_{j,k}}{(\Delta t)^2} = \left(\nabla_h^2 \psi^n\right)\Big|_{j,k} + \frac{1}{\varepsilon^2}\left(V(r_j, \theta_k) - |\psi^n_{j,k}|^2\right)\psi^n_{j,k}, \tag{3.4}$$

where ∇_h^2, the approximate differential operator for ∇^2, is defined by [6,5,34,35]

$$\begin{aligned}
\left(\nabla_h^2 \psi^n\right)|_{j,k} &= \sum_{l=-K/2}^{K/2-1} \left[D_r^2 \widehat{(\psi^n)}_l \Big|_{r=r_j} + \frac{1}{r_j} D_r \widehat{(\psi^n)}_l \Big|_{r=r_j} - \frac{l^2}{r_j^2} \widehat{(\psi^n_j)}_l \right] \mathrm{e}^{\mathrm{i}l\theta_k}, \\
D_r^2 \widehat{(\psi^n)}_l \Big|_{r=r_j} &= \frac{1}{\Delta r_j\, C_{j-1/2}} \widehat{(\psi^n_{j+1})}_l - \frac{2}{\Delta r_j\, \Delta r_{j-1}} \widehat{(\psi^n_j)}_l + \frac{1}{\Delta r_{j-1}\, C_{j-1/2}} \widehat{(\psi^n_{j-1})}_l, \\
D_r \widehat{(\psi^n)}_l \Big|_{r=r_j} &= \frac{\Delta r_{j-1}}{2\Delta r_j C_{j-1/2}} \widehat{(\psi^n_{j+1})}_l + \frac{\Delta r_j - \Delta r_{j-1}}{\Delta r_j\, \Delta r_{j-1}} \widehat{(\psi^n_j)}_l - \frac{\Delta r_j}{2\Delta r_{j-1}\, C_{j-1/2}} \widehat{(\psi^n_{j-1})}_l;
\end{aligned}$$

with $\Delta r_j = r_{j+1} - r_j$ and $C_{j-1/2} = \left(\Delta r_{j-1} + \Delta r_j\right)/2$ for $j = 0, 1, \ldots, J-1$. The initial condition (3.3) is discretized as

$$\psi^0_{j,k} = \psi_0(r_j, \theta_k), \qquad \frac{\psi^1_{j,k} - \psi^{-1}_{j,k}}{2\Delta t} = \psi_1(r_j, \theta_k), \quad 1 \le j \le J, 0 \le k \le K. \tag{3.5}$$

The boundary condition (3.2) is discretized as

$$\widehat{(\psi^n_0)}_l = (-1)^l \widehat{(\psi^n_1)}_l, \qquad \widehat{(\psi^n_J)}_l = \delta_{lm}, \quad l = -K/2, \ldots, K/2 - 1, \tag{3.6}$$

where δ_{lm} is the Kronecker delta and, for any fixed n and j, $\widehat{(\psi^n_j)}_l$ $(-K/2 \le l \le K/2 - 1)$ are the Fourier coefficients of the vector $\psi^n_{j,k}$ $(0 \le k \le K)$ defined as [34,6]

$$\widehat{(\psi^n_j)}_l = \frac{1}{K} \sum_{k=0}^{K-1} \psi^n_{j,k}\, \mathrm{e}^{-\mathrm{i}l\theta_k}, \quad -K/2 \le l \le K/2 - 1.$$

The above discretization is spectrally accurate in the θ-direction, second order accurate in both the r-direction and time. At each time step, the computational cost is $O(JK \ln K)$ since the fast Fourier transform (FFT) can be used in the θ-direction.

In our computation, we take $R = 7400$ for Ω_R and time step $\Delta t = 0.0001$. In the θ-direction, a uniform mesh with mesh size $\Delta\theta = \frac{\pi}{128}$, i.e. $K = 256$ in (3.4), is used. In the r-direction, a graded piecewise uniform mesh with 6001 grid points from the smallest mesh size $\Delta r = \frac{1}{60}$ for the subinterval $[0, 10]$ to the largest mesh size $\Delta r = \frac{11}{3}$ for the subinterval $[6400, 7400]$ is applied. These parameter values have been tested to assure the accuracy of the simulation results.

In all the figures presented below, we always use the symbol '+' to mark the center of a vortex with index $m = +1$, either '−' or '×' to mark the center of a vortex with index $m = -1$, and 'o' to mark the collision position of two or more opposite vortices.

3.2. Stability of vortex states

In order to study the stability of vortex states of NLWE numerically, we take $\varepsilon = 1$ and $V(\mathbf{x}) \equiv 1$ in (1.1) and choose the initial data (1.2) as

$$\psi_0(\mathbf{x}) = \phi_m(\mathbf{x}), \qquad \psi_1(\mathbf{x}) \equiv 0, \quad \mathbf{x} \in \mathbb{R}^2, \tag{3.7}$$

where $\phi_m(\mathbf{x})$ is given in (1.4) with $f_m(r)$ obtained numerically from (1.5) and (1.6).

As it is commonly accepted that the stability of vortices is dependent on the type of perturbations, we thus consider the stability of vortex states under a small perturbation on the initial data; an example is given by artificially setting $\psi_0(\pm 0.1, 0) = 0$.

Fig. 5 shows surface plots of $-|\psi(\mathbf{x}, t)|$ at different times for $m = 1$ and $m = 3$. From it and additional numerical experiments not shown here for brevity, we can draw the following conclusions: the vortex states with winding number $m = \pm 1$ are dynamically stable (cf. Fig. 5(a)), and resp., vortex states with winding number $|m| > 1$ are dynamically unstable in NLWE under perturbations that are either in the initial data (cf. Fig. 5(b)) or in the external potential $V(\mathbf{x})$ in (1.1). Thus, in the following sections, we only study dynamics and interaction of quantized vortices with winding numbers $m = \pm 1$ in NLWE.

4. Interaction of vortices with zero initial velocity

In this section, we report the numerical results of vortex interaction by directly simulating NLWE (1.1)–(1.3) with zero initial velocity, i.e. we take $\varepsilon = 1$ and $V(\mathbf{x}) \equiv 1$ in (1.1). The initial data is chosen as (1.8) and $\psi_1(\mathbf{x}) \equiv 0$ in (1.2).

4.1. Interactions of N $(N \ge 2)$ like vortices, Patterns I & II

Fig. 6 displays contour plots of the phase S $(\psi = \sqrt{\rho}\, \mathrm{e}^{\mathrm{i}S})$ at different times when the initial data in (1.8) is chosen as (2.6) with $N = 2$, $m_0 = +1$ and $a = 2$, and Fig. 7 shows time evolution of the vortex centers for different $N \ge 2$ in Pattern I. In addition, Figs. 8 and 9 show similar results when the initial data in (1.8) is chosen as (2.15)–(2.16) with $m_0 = +1$, i.e. Pattern II.

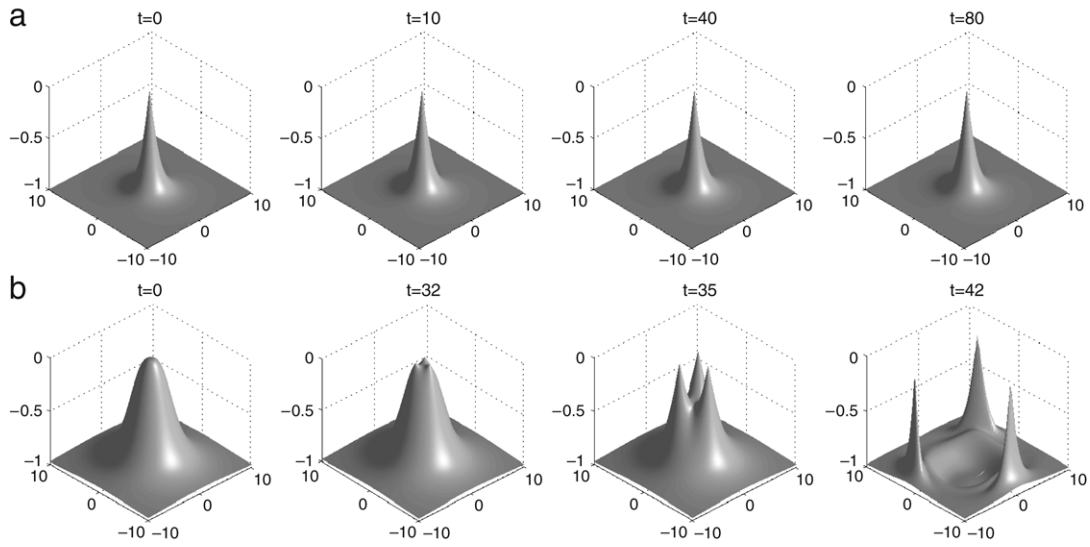

Fig. 5. Surface plots of $-|\psi(\mathbf{x}, t)|$ at different times for the stability study of the vortex states in NLWE under a perturbation on the initial data for different winding numbers: (a) $m = 1$, and (b) $m = 3$.

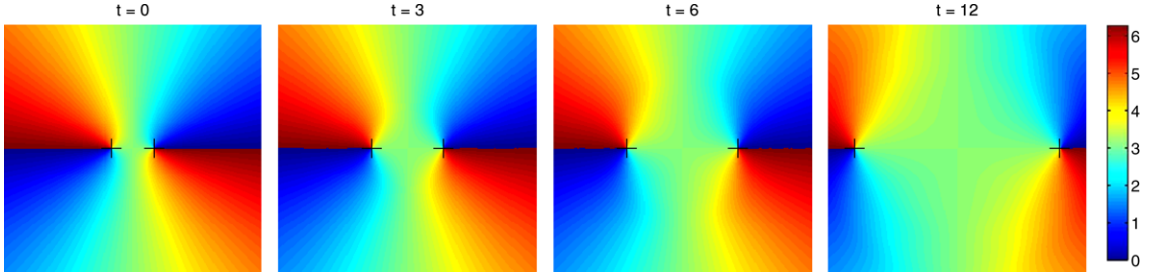

Fig. 6. Contour plots of the phase S ($\psi = \sqrt{\rho}\, e^{iS}$) at different times when the initial data is chosen as Pattern I with $N = 2$, $m_0 = +1$ and $a = 2$ in (2.6).

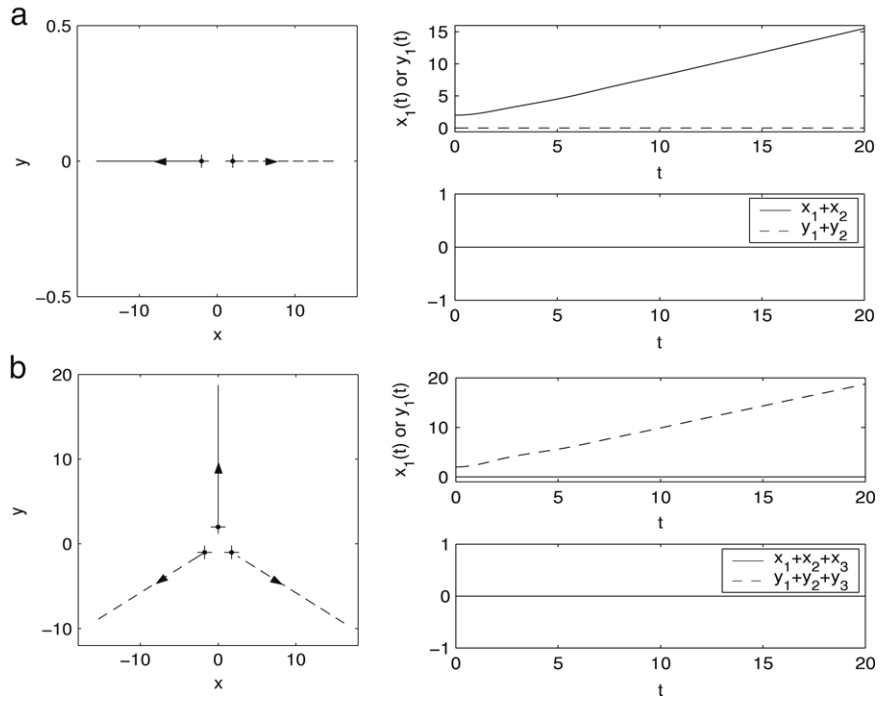

Fig. 7. Time evolution of vortex centers when the initial data is chosen as Pattern I with $m_0 = +1$ and $a = 2$ in (2.6) for different N: (a) $N = 2$, and (b) $N = 3$.

Fig. 8. Contour plots of the phase S at different times for the interaction of three like vortices in Pattern II with $N = 3$, $m_0 = +1$ and $a = 0.1$ in (2.15)–(2.16).

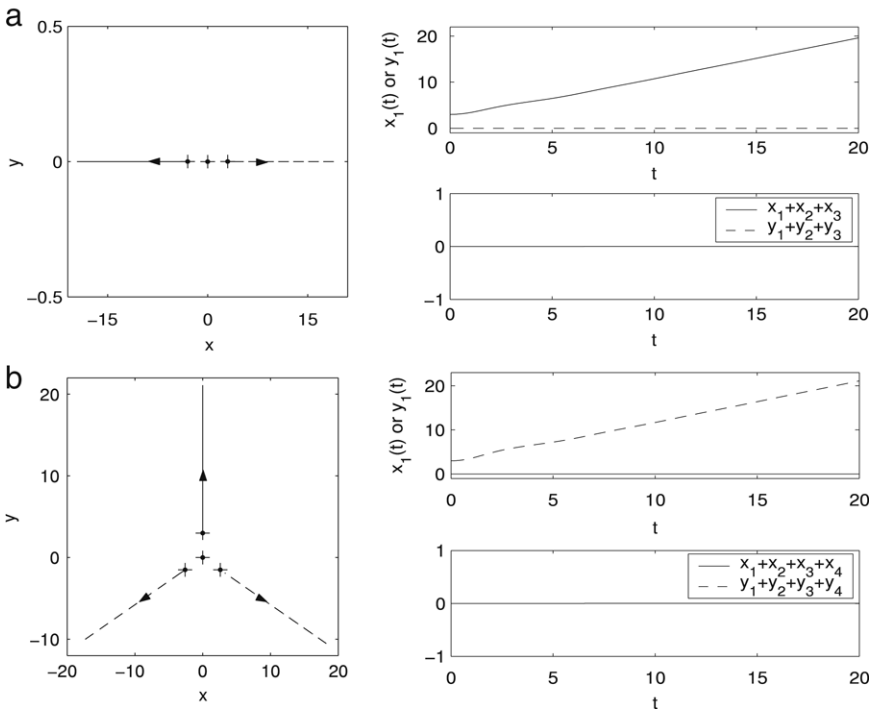

Fig. 9. Time evolution of vortex centers when the initial data is chosen as Pattern II with $m_0 = +1$ and $a = 3$ in (2.15)–(2.16) for different N: (a) $N = 3$, and (b) $N = 4$.

From Figs. 6–9 and additional numerical experiments not shown here for brevity, we can draw the following conclusions for the interaction of N like vortices when the initial data is chosen as either Pattern I or II:

(i) The mass center of the vortex centers is conserved for any time $t \geq 0$ (cf. Figs. 7 and 9), which confirms the conservation law in (2.3).

(ii) Vortices with the same index undergo a repulsive interaction and they never collide (cf. Figs. 6, 7 and 9) when they are well-separated. In Pattern II, the vortex initially at the origin does not move during the dynamics (cf. Fig. 9), which confirms the analytical solution (2.17).

(iii) Due to the symmetry of the initial data, each vortex of those initially located on a circle moves along the line passing through its initial location and the origin, and at any time $t \geq 0$, their centers are always on a circle (cf. Figs. 6–9) when they are well-separated, which confirms the analytical solutions (2.7) and (2.18).

(iv) When the distance between the vortex centers is very small at $t = 0$, i.e. they are overlapped, complicated interaction